Electroweak Nuclear Properties from Single Molecular Ions in a Penning Trap

J. Karthein,[1,*,†] S. M. Udrescu,[1,*,‡] S. B. Moroch,[1] I. Belosevic,[2] K. Blaum,[3] A. Borschevsky,[4] Y. Chamorro,[4] D. DeMille,[5,6,§] J. Dilling,[7,8] R. F. Garcia Ruiz,[1,‖] N. R. Hutzler,[9] L. F. Pašteka,[4,10] and R. Ringle[11]

[1]*Massachusetts Institute of Technology, Cambridge, Massachusetts 02139, USA*
[2]*TRIUMF, Vancouver, British Colombia V6T 2A3, Canada*
[3]*Max Planck Institute for Nuclear Physics, 69117 Heidelberg, Germany*
[4]*University of Groningen, 9747AG Groningen, The Netherlands*
[5]*Department of Physics and James Franck Institute at the University of Chicago, Chicago, Illinois 60637, USA*
[6]*Physics Division at Argonne National Laboratory, Lemont, Illinois 60439, USA*
[7]*Duke University, Durham, North Carolina 27708, USA*
[8]*Oak Ridge National Laboratory, Oak Ridge, Tennessee 37830, USA*
[9]*California Institute of Technology, Pasadena, California 91125, USA*
[10]*Comenius University, 84215 Bratislava, Slovakia*
[11]*Facility for Rare Isotope Beams, East Lansing, Michigan 48824, USA*

(Received 18 October 2023; revised 31 January 2024; accepted 18 April 2024; published 19 July 2024)

We present a novel technique to probe electroweak nuclear properties by measuring parity violation (PV) in single molecular ions in a Penning trap. The trap's strong magnetic field Zeeman shifts opposite-parity rotational and hyperfine molecular states into near degeneracy. The weak interaction-induced mixing between these degenerate states can be larger than in atoms by more than 12 orders of magnitude, thereby vastly amplifying PV effects. The single molecule sensitivity would be suitable for applications to nuclei across the nuclear chart, including rare and unstable nuclei.

DOI: 10.1103/PhysRevLett.133.033003

Introduction—Of nature's four known fundamental forces, the weak force is the only one known to violate parity (P) and charge-parity (CP) symmetry. In this context, precision studies of the weak interaction provide powerful tests of the standard model, violations of the fundamental symmetries, and the existence of new physics [1–3]. Accelerator-based experiments and atomic parity violation studies have provided key insights into the weak interaction between the electrons and nucleons, mediated by Z^0-boson exchange [4–6]. However, the electroweak interactions between nucleons are only poorly understood [7–12]. A clear disagreement exists between measurements [1,13,14].

Recent progress in precision control and interrogation of molecules has demonstrated powerful routes for precision studies of symmetry-violating properties [1,15–18]. Parity violation (PV) can produce unique signatures in the molecular energy levels, enabling the isolation of weak force effects from the overwhelmingly dominant strong and electromagnetic forces [19–21]. The proximity of opposite parity molecular levels provides high sensitivity to symmetry-violating properties, which can be several orders of magnitude larger than in atomic systems. Moreover, external magnetic fields can drive these opposite-parity states into near degeneracy, enhancing their sensitivity to PV properties [22]. The possibility of about 11 orders of magnitude of enhancement of PV-induced state mixing was recently demonstrated with a neutral beam of ^{138}BaF [23].

In this Letter, we propose and analyze a new method for measuring PV nuclear properties using single molecular ions and a Penning trap, which allows for long coherence times ($\gg$1 ms) [20]. Combined with its well-controlled electric and magnetic fields, an enhancement in excess of 12 orders of magnitude in PV-induced state mixing relative to atoms can be achieved, thereby vastly increasing sensitivity to electroweak nuclear properties. The precision and versatility of our technique will enable measurements of many isotopes across the nuclear chart. These include species that may be difficult to manipulate and measure in neutral forms, such as short-lived nuclei [18,24,25].

In a diatomic molecule, PV properties are dominated by the nuclear-spin-dependent PV (NSD-PV) interactions. These primarily arise from the electron-vector and nucleon axial-vector (V_eA_N) Z^0-boson exchange [1], and the electron electromagnetic interaction with the nuclear anapole moment [1,26,27] (so far only detected in ^{133}Cs [4]). Another contribution could come from new interactions beyond the standard model between electrons and nucleons, mediated by yet-to-be-discovered gauge bosons [28–30].

Our proposed method should be highly general for various molecular ions. However, we will focus on $^{29}SiO^+$ due to practical and theoretical advantages for the initial demonstration: Its rotational and electronic structure is known [31], the ground electronic state is $^2\Sigma^+$, and it was demonstrated suitable for laser cooling [32,33].

§Corresponding author: ddemille@uchicago.edu
‖Corresponding author: rgarciar@mit.edu

Effective Hamiltonian and electroweak properties—Our scheme builds on the concepts introduced in [20,34]. The effective Hamiltonian describing the lowest rotational and hyperfine energy levels of $^{29}SiO^+$, in the absence of PV effects, can be expressed as

$$H_0 = B_0 N^2 + D_0 N^4 + \gamma \boldsymbol{N}\cdot\boldsymbol{S} + b\boldsymbol{I}\cdot\boldsymbol{S} + c(\boldsymbol{I}\cdot\boldsymbol{n})(\boldsymbol{S}\cdot\boldsymbol{n}),$$

with $\boldsymbol{N} = \boldsymbol{R} + \boldsymbol{L}$, where $\boldsymbol{R}$ is the mechanical rotation of the molecular framework, $\boldsymbol{L}$ is the orbital angular momentum of the electron, $\boldsymbol{S}$ and $\boldsymbol{I}$ are the molecular frame electron and nuclear spin operator, respectively, and $\boldsymbol{n}$ is the unit vector along the internuclear axis. The rotational, centrifugal distortion, and spin-rotational constants are B_0, D_0, and γ. b and c are hyperfine structure constants associated with the ^{29}Si nucleus. The rotational constant of $^{29}SiO^+$ is far larger than all the other molecular parameters in H_0 [35]. Thus, N is a good quantum number for levels of energy $E_N \approx B_0 N(N+1)$ and parity $P_N = (-1)^N$.

When a magnetic field of a particular magnitude B is applied (see Fig. 1), sublevels of the $N^P = 0^+$ and 1^- states can be Zeeman shifted close to degeneracy. For $^{29}SiO^+$, this magnetic field strength is $B \approx [(E_1 - E_0)/2\mu_B] \approx 1.5$ T, since the coupling to the electron spin S dominates the Zeeman shift via the Hamiltonian $H_Z = -g\mu_B \boldsymbol{S}\cdot\boldsymbol{B}$ with g factor $g \approx -2$, the Bohr magneton μ_B, and the magnetic field aligned with the z axis $\boldsymbol{B} = B\boldsymbol{z}$ [23]. This field is strong enough to decouple $\boldsymbol{S}$ from $\boldsymbol{I}$ and $\boldsymbol{N}$. Hence, the rotational and hyperfine levels are better described in the decoupled basis used for the rest of the Letter: $|N, m_N\rangle|S, m_S\rangle|I, m_I\rangle$.

The NSD-PV interactions can mix opposite-parity levels. The Hamiltonian $H_{\mathrm{PV}} = \kappa'(G_F/\sqrt{2})(\boldsymbol{\alpha}\boldsymbol{I}/I)\rho(\boldsymbol{r})$ [26] describes such PV interactions, where κ' includes all the NSP-PV contributions. We denote the Fermi constant G_F, Dirac matrices vector $\boldsymbol{\alpha}$, nuclear spin $\boldsymbol{I}$, and nuclear density with respect to the nuclear center $\rho(\boldsymbol{r})$. An effective Hamiltonian acting only within the subspace of rotational and hyperfine levels can be obtained by averaging the previous Hamiltonian over the electronic wave function, given by $H_{\mathrm{eff}} = \kappa' W_{\mathrm{A}} C$, where W_{A} is a matrix element that includes the expectation value of H_{PV} over the electronic wave function in the $^2\Sigma$ state in the rotating frame of the molecule, which can be computed numerically using state-of-the-art quantum chemistry methods with uncertainties as low as a few percent [38]. $C = \{[(\boldsymbol{n}\times\boldsymbol{S})\cdot\boldsymbol{I}]/I\}$ contains the angular momentum dependence of H_{eff} and its matrix elements can be calculated analytically using angular momentum algebra [21].

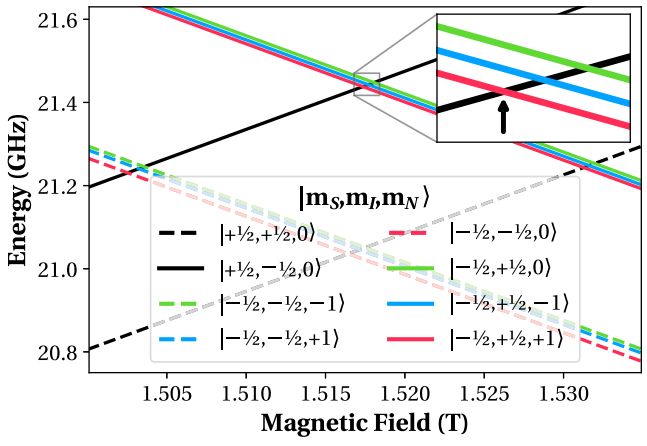

FIG. 1. Calculated energies of opposite parity rotational and hyperfine states in $^{29}SiO^+$ for different magnetic field strengths, based on the Hamiltonian H_0 and parameters given in [36,37]. The positive parity states $|\Psi^+_\uparrow\rangle$ are rising, while the negative ones $|\Psi^-_\downarrow\rangle$ are descending. For details, see text.

Measurement strategy—Our proposed experiment will be performed in a Penning ion trap. This device is widely used in precision atomic and nuclear physics [39–42]. The trap consists of a strong magnetic and a weak electrostatic field, allowing three-dimensional trapping of ions (see Ref. [43] for a review on Penning traps). We use the trapping magnetic field to Zeeman shift two opposite parity states into near degeneracy (see arrow in Fig. 1). Moreover, the intrinsic trap design allows for various magnetic field strengths for maximal flexibility in the choice of ion species and rotational-hyperfine states.

Our experimental principle is identical to the one for neutral molecules in Refs. [20,23]. In the presence of axial (i.e., aligned with the magnetic field) and radial electric fields, E_z and E_r, the effective Hamiltonian of this two-level system is

$$H_\pm = \begin{pmatrix} \alpha_r E_r^2 + \alpha_z E_z^2 & iW + d\cdot E_z \\ -iW + d\cdot E_z & \Delta \end{pmatrix},$$

with the weak interaction matrix element $iW(m'_N, m'_I, m_N, m_I) \equiv \kappa' W_{\mathrm{A}} \langle \Psi^-_\downarrow(m'_N, m'_I)|C|\Psi^+_\uparrow(m_N, m_I)\rangle$, the expectation value d of the dipole moment operator, $\boldsymbol{D}$, between the two levels and the general wave function, $|\Psi(t)\rangle = c_+(t)|\Psi^+_\uparrow\rangle + e^{-i\Delta t}c_-(t)|\Psi^-_\downarrow\rangle$, of the two-level system with its eigenstates $|\Psi^P_{m_S}\rangle$ of parity P and spin projection m_S, and its time-dependent amplitudes $c_P(t)$ [see Refs. [20,23,44–46] and the Supplemental Material (SM)-B [47] for details]. Δ is a small detuning of the two levels from perfect degeneracy and depends on the applied magnetic field strength B; α_r and α_z represent the radial and axial contributions to the differential polarizability of the two levels [48], while E_r and E_z are any external radial and axial E fields.

In the ideal case of a single ion resting in a stable magnetic field B at $t_0 = 0$ with zero external electric fields prepared in the $|\Psi^+_\uparrow\rangle$ state in the center of our trap, we measure W using the Stark-interference procedure described

in Ref. [20]. Thereby, population transfer from the initial positive $|\Psi^+_\uparrow\rangle$ to the negative $|\Psi^-_\downarrow\rangle$ parity state occurs due to the PV matrix element and the interaction with a sinusoidal electric field. We repeat this measurement for several N_0 ions to determine the population transfer probability by measuring the average signal $S = N_0|c_-(t)|^2$ (see SM-B [47] and Refs. [44–46] for details). The existence of parity violation leads to a nonzero asymmetry, defined as $A_{\mathrm{PV}} \equiv \{[S(+E_{\mathrm{ext}}) - S(-E_{\mathrm{ext}})]/[S(+E_{\mathrm{ext}}) + S(-E_{\mathrm{ext}})]\}$ [23], where $S(+E_{\mathrm{ext}})$ and $S(-E_{\mathrm{ext}})$ refer to the signals obtained for measurements with zero (+) and π (−) phase shift in the sinusoidal field.

For $^{29}\mathrm{SiO}^+$, the population transfer and, hence, the asymmetry can be estimated using first-order perturbation theory (see SM-B [47] and Refs. [44–46] for details). For interrogation times $t_x \approx (2\pi N/\omega_{\mathrm{ext}}) \approx (\pi/\Delta)$ at integer N, the PV asymmetry becomes [20]

$$A_{\mathrm{PV}} = \frac{\frac{2W}{\Delta}\cdot\frac{\Omega_R}{\omega_{\mathrm{ext}}}}{(\frac{W}{\Delta})^2 + (\frac{\Omega_R}{\omega_{\mathrm{ext}}})^2}, \tag{1}$$

with $\Omega_R = dE_{\mathrm{ext}}$. Ultimately, W is determined via the population transfer probability for different values of Δ, i.e., magnetic field strengths B we can easily scan in our setup. Its statistical uncertainty is

$$\delta W = \frac{\Delta}{4\sqrt{2N_0}\sin(\frac{\Delta t_x}{2})}\frac{\sqrt{\eta^2+1}}{\eta} \tag{2}$$

using $\eta \equiv (\Omega_R/\omega_{\mathrm{ext}})/(W/\Delta)$ for the number of molecules N_0.

To reduce δW, we want to minimize Δ. Since we are technically limited in arbitrarily reducing Δ (as discussed in the following section), we set the interrogation time to $t_x = (\pi/\Delta)$ once Δ is minimized. Thus, the precise control of the interrogation time t_x in our trap for a minimal uncertainty on δW and precise variation of t_x to check for systematic effects, are clear advantages we can leverage over experiments performed on molecular beams.

From our measurement of W and the calculated W_A and C, we can extract $\kappa' \approx \kappa'_2 + \kappa'_a$, encoding the physics of the weak interaction that leads to NSD-PV: κ'_2, arising from the $V_e A_N$ term in the electron-nucleon-Z^0-boson exchange, and the electron electromagnetic interaction with the anapole moment, κ'_a. Applying our technique to a wide range of isotopic chains, including radioactive ones [18,24,25], could allow for a separation of κ'_2 and κ'_a based on the dependence of κ'_a on the nuclear mass A and spin I [20,27].

Experimental details—Trapped ions in a Penning trap move on three superimposed eigenmotions inside the trap. The eigenmotions' frequency, phase, and amplitude can be controlled and coupled through radio-frequency excitations on the ion trap's electrodes [43]. The eigenmotions can be further cooled by coupling to a resonance circuit at 1K. Once the ion is located in the trap center in equilibrium with the 1-K environment, it is decoupled from the resonance circuit using a cryogenic switch. It remains in a nominally zero E_{ext} field, allowing for the above assumptions on the Hamiltonian due to low reheating rates of ~ 65 mK/s [49].

An additional, significant advantage of our proposed method is that the magnetic field strength B experienced by the molecular ion with charge-to-mass ratio q/m can be precisely determined through a cyclotron frequency $\nu_c = (Bq/2\pi m)$ determination to the 10^{-11} level of precision or better [50,51].

In our proposed setup, neutral $^{29}\mathrm{SiO}$ molecules are produced by laser ablating a silicon rod in the supersonic expansion of a mixture of oxygen and argon gas [52]. The molecules are photoionized using resonant laser light [53] into the ground electronic and vibrational states populating only low rotational levels [54]. The measurement scheme shown in Fig. 2 works as follows:

(i) The molecular ions are trapped in the Penning trap, and a single molecule is selected using the evaporative cooling technique [55]. Once the ion is located at the trap center in equilibrium with the 1-K environment (assumed as the kinetic temperature of the ions moving forward) and decoupled from the resonant circuit, it is optically pumped into its rotational ground state [94(3)% fidelity were shown in Ref. [32] for $^{28}\mathrm{SiO}^+$]. This level is further split into four hyperfine substates. Given the large splitting between these substates (>100 MHz), they can be addressed individually after the rotational cooling using lasers or microwaves to transfer the population to the state of interest, $|\Psi^+_\uparrow\rangle$ (Fig. 1, solid black line), with >90% fidelity.

(ii) To ensure the molecule is not in the negative parity state $|\Psi^-_\downarrow\rangle$ (Fig. 1, colored lines) even after the state transfer, the molecule in $|\Psi^-_\downarrow\rangle$ is state-selectively dissociated via excitation to a higher-lying autodissociating state [32]. The timescale for this process is ∼10 ns, i.e., short compared to all inverse frequencies in this measurement; thus, it corresponds to an instantaneous (but conditional) quantum projection onto unaffected states.

(iii) This step constitutes the starting point of the measurement. It will be executed after step (i) and in

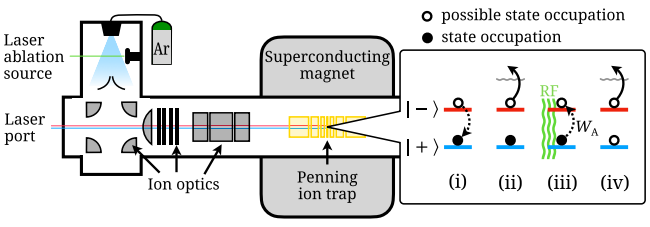

FIG. 2. Schematic layout and measurement principle with a laser port for the ionization, cooling, and dissociation lasers. Our measurement procedure, (i)–(iv), is described in the text.

parallel to step (ii) since $|\Psi^+_\uparrow\rangle$ would start to evolve in time even without an external electric field.

To induce Stark mixing, we have the ion experience, a sinusoidal electric field $E_z(t) = E_{\text{ext}} \cdot \sin(\omega_{\text{ext}} t)$ with $E_{\text{ext}} \approx 6$ V/cm and $\Omega_R/2\pi \approx 3$ kHz in its rest frame. This is achieved by exciting the ion to an axial amplitude of ~0.3 mm in the harmonic trapping potential with a ~20 V single cycle, resonant sinusoidal-wave "kick" to the trap's end caps as routinely achieved in practice [56].

(iv) The final state detection is performed by molecular dissociation of the negative parity state $|\Psi^-_\downarrow\rangle$, using the same autoionizing state as in step (ii) as soon as the oscillating field in step (iii) is switched "off" by reversing the sinusoidal "kick." Since the dissociation process is parity-state selective, we can perform a "double-dip" mass measurement [56] in search of $^{29}SiO^+$, $^{29}Si^+$, or $^{16}O^+$ as a measurement of the final parity state. If a dissociation had occurred, we can remove the $^{29}Si^+$ or $^{16}O^+$ ion from the trap and load a new $^{29}SiO^+$ ion. If no dissociation occurs, the measurement is restarted at step (i).

Figure 3 shows the simulated PV asymmetry, A_{PV}, in Eq. (1), as a function of Δ for a range of possible W values. For $^{29}SiO^+$, we assume $\Omega_R/2\pi = 3$ kHz, $\omega_{\text{ext}}/2\pi = 350$ kHz, and scan $\Delta/2\pi$ ranging from -150 Hz to 150 Hz in steps of 50 Hz. Measuring different values of Δ was shown to be effective in avoiding various systematic uncertainties [23,57]. Measuring at other relevant level crossings will also allow diagnosing systematics.

Heavier molecules with larger weak matrix elements comparable to Δ ($W \gtrsim 100$ Hz), such as the potentially laser-coolable TlF^+ [58] (see Table I), do not require additional external Stark mixing for amplifying the sought signal. As suggested in Ref. [34], the level crossing shown in Fig. 1 turns into a pseudocrossing, which can be measured directly. This approach requires an advanced level of systematic control which we plan to investigate in the future.

Uncertainty estimates—Here, we estimate the primary sources and magnitude of uncertainty for $^{29}SiO^+$ with the

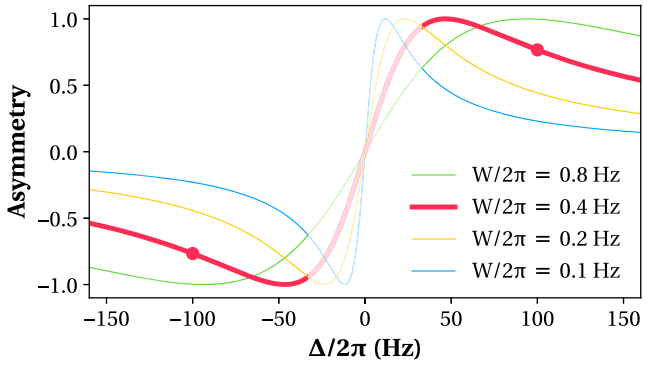

FIG. 3. Asymmetry for $^{29}SiO^+$ for different W and Δ. The assumed experimental condition is indicated in red with details provided in the text. The red dots show the expected asymmetry at $\Delta/2\pi = \pm 100$ Hz.

calculated $W_A/2\pi = 16$ Hz from Table I, corresponding to $W/2\pi = 0.4$ Hz when assuming $\kappa' = 0.05$ and $C = 0.5$.

(i) Initial axial amplitude: The main contribution to the systematic uncertainty is expected to come from the ac Stark shift of the energy levels of interest due to the transverse and axial components of the electric field, with the effects proportional to $\alpha_r E_r^2$ and $\alpha_z E_z^2$, respectively. The uncertainty associated with this shift arising from the thermal distribution of ion positions and velocities is expected to be $\delta\Delta/2\pi \approx 30$ Hz (see SM-A [47] for details of the calculations). To clearly tell apart the two opposite parity levels of interest, we assume moving forward a value of $\Delta/2\pi \approx 100$ Hz, and therefore $t_x = \pi/\Delta = 5$ ms to minimize δW, leading to a maximum state transfer probability of the positive parity state's population of ~0.06% and an asymmetry of ~0.75 (red dots in Fig. 3).

A second major source of uncertainty is expected to derive from the thermal noise in the initial axial amplitude of cooled ions. Once cooled and resting in the center of the Penning trap, the ions' energy is Boltzmann distributed with an average initial axial amplitude of $z_0 = \sqrt{[2k_b T d_{\text{char}}^2/(q_{\text{ion}} U_0 C_2)]}$, where k_b is the Boltzmann constant, q_{ion} is the electron charge e, and we assume $T = 1$ K. Based on our trap design [56] optimized for E-field homogeneity of the electric trapping potential of depth $U_0 = -35$ V, characteristic trap length $d_{\text{char}} = \sqrt{0.5(z_{\text{trap}}^2 + r_{\text{trap}}^2/2)} = 3$ mm (with the central ring electrode's length z_{trap} and radius r_{trap}), and the dimensionless quadrupole constant $C_2 = -0.6$. The initial axial motion is then $z_0 \approx 10$ μm, which would result in an average thermal noise of $\delta E_{\text{th}} \approx 0.2$ V/cm, corresponding to $\delta W/W \approx 3\%$ for $^{29}SiO^+$. Both of these effects are statistical, i.e., they can be reduced by increasing the number of measurements.

(ii) Magnetic field: Short-term magnetic field instabilities (for the measurement time of up to many milliseconds) are expected to be $\delta B/B \lesssim 10^{-10}$ [59,60]. Observed temporal changes in the magnetic field tracked in a neighboring trap center will be used for live adjustment of slow magnetic field drifts on top of typical temperature and pressure stabilization of the magnet [56]. With this method, we anticipate $\delta B/B \approx 10^{-10}$ for the duration of the data taking [61]. Furthermore, deviations from spatial uniformity due to higher-order field effects not accounted for by shimming coils are expected to be $\delta B/B < 10^{-10}$ for the small probed volume of $\ll 0.1$ mm^3 [56]. All of these effects can be quantified based on precise measurements of ν_c for well-known species. These effects lead to a total systematic uncertainty from the magnetic field of $\delta B/B \approx 10^{-10}$, or $\delta\Delta/2\pi \approx 4$ Hz, i.e., $\delta W/W \approx 4\%$ for $^{29}SiO^+$.

(iii) Electric field: A relative electric field uncertainty of $\delta E/E \ll 1\%$, which can be routinely achieved in practice [56], would have negligible effect on δW.

TABLE I. Diatomic molecular ions with sizable weak matrix elements W_A (of the first-mentioned atom) in units of Hz and their bond lengths BL in units of Å. Data on additional molecular ions can be found in [62]. For details, see text.

System	W_A	BL	System	W_A	BL	System	W_A	BL
$^{11}B^{19}F^+$	1	1.21	$^{227}Ac^{79}Br^+$	1644	2.72	$^{261}Lr^{1}H^+$	11 295	1.89
$^{29}Si^{16}O^+$	13	1.52	$^{227}Ac^{127}I^+$	1677	2.94	$^{261}Lr^{7}Li^+$	2745	3.49
$^{205}Tl^{19}F^+$	4472	1.98	$^{229}Th^{16}O^+$	2506	1.8	$^{261}Lr^{19}F^+$	8826	1.93
$^{227}Ac^{1}H^+$	1649	2.23	$^{229}Th^{32}S^+$	1752	2.31	$^{261}Lr^{23}Na^+$	2425	3.8
$^{227}Ac^{19}F^+$	1655	2.08	$^{229}Th^{80}Se^+$	1588	2.45	$^{261}Lr^{35}Cl^+$	10 158	2.35
$^{227}Ac^{35}Cl^+$	1632	2.56	$^{229}Th^{126}Te^+$	1323	2.68	$^{261}Lr^{39}K^+$	1658	4.26

We thus anticipate a total systematic uncertainty of $\delta W/W < 5\%$ for $^{29}SiO^+$. To achieve a 10% statistical uncertainty on the proposed measurement, we need on the order of 10^5 trapped molecular ions. Given a measurement cycle of a few seconds (dominated by mass selection, cooling, and state preparation), a 10% relative uncertainty measurement would thus be feasible in about one week of measurement time for $^{29}SiO^+$.

Calculated sensitivity factors—We calculated the molecular matrix element of the anapole moment W_A for the $^2\Sigma_{1/2}$ ground states of BF^+, $^{29}SiO^+$, and TlF^+ at the four-component relativistic Fock-space coupled-cluster (FSCC) level of theory using the finite field approach. This formalism includes H_{PV} as a perturbation to the Dirac-Coulomb Hamiltonian. The W_A factor is obtained as the first derivative of the total energy to this perturbation [38]. We used the dyall.cv4z basis sets [63,64] and correlated 13 (all), 21 (all), and 51 electrons for BF^+, $^{29}SiO^+$, and TlF^+, respectively. A Gaussian charge distribution represented the nucleus.

Furthermore, we calculated W_A for Ac, Th, and Lr-containing molecular ions. Here, we used the four-component relativistic Dirac-Hartree-Fock (DHF) level of theory. In this case, W_A was extracted from the off-diagonal matrix elements of the operator $\alpha\rho(r)$ acting on the degenerate $\Omega = |\pm 1/2\rangle$ states in the molecular spinor basis. We employed the dyall.cv4z basis set for all the elements [63–66].

The molecular geometries were optimized at the exact two-component [67,68] coupled-cluster level of theory, including single and double excitations in the parallel implementation of the Dirac program package [69]. The cutoff was set to −20 to 30 a.u. We used the dyall.v3z basis sets [64–66] for all the systems, except for $^{29}SiO^+$ (experimental bond length [70]), and BF^+/TlF^+ (s-aug-dyall.v4z basis sets [63,64]). All results are presented in Table I.

Besides $^{29}SiO^+$ [31–33], spectroscopic information in the literature among the presented molecular ions is not available to the best of our knowledge. Hence, prior studies of each molecular ion are necessary to find the needed rotational-hyperfine parameters and laser-cooling transitions.

Outlook—We proposed a new technique that can provide a highly sensitive route to investigate yet-to-be-explored nuclear parity-violating properties using single molecular ions. These measurements will enable stringent tests of the weak interaction in stable and short-lived isotopes across the nuclear chart. This technique could be directly applied to light isotopes, for which PV nuclear properties can already be calculated on the lattice [71,72] and with *ab initio* methods [73]. For diatomic molecules containing elements as light as the deuteron, challenges with the required magnetic field strength could be overcome by using ground-rotational states in polyatomic molecules [20,25,74]. Furthermore, applying advanced cooling techniques already demonstrated in Penning traps would enable reducing the trapped molecule's kinetic energy to ∼1–100 mK [75–79], resulting in a reduction of the uncertainty on W by 1 to 2 orders of magnitude.

Acknowledgments—This work was supported by the U.S. Department of Energy (DOE), Office of Science (OS), and Office of Nuclear Physics under Awards No. DE-SC0021176 and No. DE-SC0021179. This research is partly based on work supported by Laboratory Directed Research and Development (LDRD) funding from Argonne National Laboratory, provided by the OS Director of the U.S. DOE under Contract No. DE-AC02-06CH11357. We thank the Center for Information Technology of the University of Groningen for its support and access to the Peregrine high-performance computing cluster. The INCITE program awarded computer time. This research also used resources from the Oak Ridge Leadership Computing Facility, a DOE-OS User Facility supported under Contract No. DE-AC05-00OR22725. We also acknowledge the support from High Sector Fock space coupled cluster method: benchmark accuracy across the periodic table (with Project No. VI.Vidi.192.088 of the research program Vidi, financed by the Dutch Research Council) and the 2020 Incite Award: "PRECISE: Predictive Electronic Structure Modeling of Heavy Elements." J. K. acknowledges the support of a Feodor Lynen Fellowship of the Alexander-von-Humboldt Foundation. S. B. M. acknowledges the support of a National Science Foundation Graduate Research Fellowship (NSF Grant No. 2141064)

and a Fannie and John Hertz Graduate Fellowship. The work of A. B. was supported by the project "High Sector Fock space coupled cluster method: benchmark accuracy across the periodic table" with Project No. Vi.Vidi.192.088 of the research program Vidis, financed by the Dutch Research Council (NWO). L. F. P. acknowledges the support from NWO Project No. VI.C.212.016 of the talent program VICI, and the support from the Slovak Research and Development Agency (Projects No. APVV-20-0098, No. APVV-20-0127). All sensitivity factor calculations were performed using an adapted version of the Dirac program package [80,81]. Simulations used NUMPY [82], SCIPY [83], PANDAS [84,85], and SIMION [86]. Figures were produced using MATPLOTLIB [87].

[1] M. S. Safronova, D. Budker, D. DeMille, D. F. J. Kimball, A. Derevianko, and C. W. Clark, Search for new physics with atoms and molecules, Rev. Mod. Phys. **90**, 025008 (2018).

[2] H. Davoudiasl, H.-S. Lee, and W. J. Marciano, "Dark" z implications for parity violation, rare meson decays, and Higgs physics, Phys. Rev. D **85**, 115019 (2012).

[3] P. Langacker, The physics of heavy Z' gauge bosons, Rev. Mod. Phys. **81**, 1199 (2009).

[4] C. Wood, S. Bennett, D. Cho, B. Masterson, J. Roberts, C. Tanner, and C. E. Wieman, Measurement of parity nonconservation and an anapole moment in cesium, Science **275**, 1759 (1997).

[5] The Jefferson Lab PVDIS Collaboration, Measurement of parity violation in electron–quark scattering, Nature (London) **506**, 67 (2014).

[6] D. Androić *et al.* (Qweak Collaboration), Parity-violating inelastic electron-proton scattering at low Q^2 above the resonance region, Phys. Rev. C **101**, 055503 (2020).

[7] B. Desplanques, J. F. Donoghue, and B. R. Holstein, Unified treatment of the parity violating nuclear force, Ann. Phys. (N.Y.) **124**, 449 (1980).

[8] E. G. Adelberger and W. C. Haxton, Parity violation in the nucleon-nucleon interaction, Annu. Rev. Nucl. Part. Sci. **35**, 501 (1985).

[9] W. C. Haxton and B. R. Holstein, Hadronic parity violation, Prog. Part. Nucl. Phys. **71**, 185 (2013), fundamental Symmetries in the Era of the LHC.

[10] S. Gardner, W. Haxton, and B. R. Holstein, A new paradigm for hadronic parity nonconservation and its experimental implications, Annu. Rev. Nucl. Part. Sci. **67**, 69 (2017).

[11] J. de Vries, E. Epelbaum, L. Girlanda, A. Gnech, E. Mereghetti, and M. Viviani, Parity- and time-reversal-violating nuclear forces, Front. Phys. **8**, 218 (2020).

[12] S. Gardner and G. Muralidhara, Toward a unified treatment of $\delta\,\mathrm{s} = 0$ parity violation in low-energy nuclear processes, Phys. Rev. C **107**, 055501 (2023).

[13] M. J. Ramsey-Musolf and S. A. Page, Hadronic parity violation: A new view through the looking glass, Annu. Rev. Nucl. Part. Sci. **56**, 1 (2006).

[14] B. R. Holstein, Overview of hadronic parity violation, Eur. Phys. J. A **32**, 505 (2007).

[15] V. Andreev, D. G. Ang, D. DeMille, J. M. Doyle, G. Gabrielse, J. Haefner, N. R. Hutzler, Z. Lasner, C. Meisenhelder, B. R. OLeary, C. D. Panda, A. D. West, E. P. West, and X. Wu (ACME Collaboration), Improved limit on the electric dipole moment of the electron, Nature (London) **562**, 355 (2018).

[16] W. B. Cairncross, D. N. Gresh, M. Grau, K. C. Cossel, T. S. Roussy, Y. Ni, Y. Zhou, J. Ye, and E. A. Cornell, Precision measurement of the electron's electric dipole moment using trapped molecular ions, Phys. Rev. Lett. **119**, 153001 (2017).

[17] T. S. Roussy, L. Caldwell, T. Wright, W. B. Cairncross, Y. Shagam, K. B. Ng, N. Schlossberger, S. Y. Park, A. Wang, J. Ye, and E. A. Cornell, A new bound on the electron's electric dipole moment, Science **381**, 46 (2023).

[18] R. F. Garcia Ruiz *et al.*, Spectroscopy of short-lived radioactive molecules, Nature (London) **581**, 396 (2020).

[19] O. Sushkov and V. Flambaum, Parity breaking effects in diatomic molecules, Zh. Eksp. Teor. Fiz. **75**, 1208 (1978), http://www.jetp.ras.ru/cgi-bin/e/index/e/48/4/p608?a=list.

[20] D. DeMille, S. B. Cahn, D. Murphree, D. A. Rahmlow, and M. G. Kozlov, Using molecules to measure nuclear spin-dependent parity violation, Phys. Rev. Lett. **100**, 023003 (2008).

[21] V. Flambaum and I. Khriplovich, On the enhancement of parity nonconserving effects in diatomic molecules, Phys. Lett. A **110**, 121 (1985).

[22] M. G. Kozlov and L. N. Labzowsky, Parity violation effects in diatomics, J. Phys. B **28**, 1933 (1995).

[23] E. Altuntaş, J. Ammon, S. B. Cahn, and D. DeMille, Demonstration of a sensitive method to measure nuclear-spin-dependent parity violation, Phys. Rev. Lett. **120**, 142501 (2018).

[24] S. M. Udrescu *et al.*, Isotope shifts of radium monofluoride molecules, Phys. Rev. Lett. **127**, 033001 (2021).

[25] G. Arrowsmith-Kron *et al.*, Opportunities for fundamental physics research with radioactive molecules, arXiv:2302.02165.

[26] V. Flambaum and I. Khriplovich, P-odd nuclear forces: A source of parity violation in atoms, Sov. Phys. JETP **52**, 835 (1980), http://www.jetp.ras.ru/cgi-bin/e/index/e/52/5/p835?a=list.

[27] V. Flambaum, I. Khriplovich, and O. Sushkov, Nuclear anapole moments, Phys. Lett. B **146**, 367 (1984).

[28] V. A. Dzuba, V. V. Flambaum, and Y. V. Stadnik, Probing low-mass vector bosons with parity nonconservation and nuclear anapole moment measurements in atoms and molecules, Phys. Rev. Lett. **119**, 223201 (2017).

[29] Y. Stadnik and V. Flambaum, Nuclear spin-dependent interactions: searches for WIMP, axion and topological defect dark matter, and tests of fundamental symmetries, Eur. Phys. J. C **75**, 110 (2015).

[30] Y. V. Stadnik and V. V. Flambaum, Axion-induced effects in atoms, molecules, and nuclei: Parity nonconservation, anapole moments, electric dipole moments, and spin-gravity

and spin-axion momentum couplings, Phys. Rev. D **89**, 043522 (2014).
[31] P. R. Stollenwerk, B. C. Odom, D. L. Kokkin, and T. Steimle, Electronic spectroscopy of a cold SiO^+ sample: Implications for optical pumping, J. Mol. Spectrosc. **332**, 26 (2016).
[32] P. R. Stollenwerk, I. O. Antonov, S. Venkataramanababu, Y.-W. Lin, and B. C. Odom, Cooling of a zero-nuclear-spin molecular ion to a selected rotational state, Phys. Rev. Lett. **125**, 113201 (2020).
[33] J. H. V. Nguyen and B. Odom, Prospects for doppler cooling of three-electronic-level molecules, Phys. Rev. A **83**, 053404 (2011).
[34] M. Kozlov, L. Labzovski, and A. Mitrushchenko, Parity nonconservation in diatomic molecules in a strong constant magnetic field, Zh. Éksp. Teor. Fiz. **100**, 749 (1991), http://www.jetp.ras.ru/cgi-bin/e/index/e/73/3/p415?a=list.
[35] G.-Z. Zhu, G. Lao, C. Ho, W. C. Campbell, and E. R. Hudson, High-resolution laser-induced fluorescence spectroscopy of $^{28}Si^{16}O^+$ and $^{29}Si^{16}O^+$ in a cryogenic buffer-gas cell, J. Mol. Spectrosc. **384**, 111582 (2022).
[36] L. B. Knight Jr, A. Ligon, R. Woodward, D. Feller, and E. R. Davidson, The generation and trapping of the high-temperature oxosilyliumyl cation radicals ($^{28}SiO^+$ and $^{29}SiO^+$) in neon matrixes at 4 K; an ESR and *ab initio* CI theoretical investigation, J. Am. Chem. Soc. **107**, 2857 (1985).
[37] G.-Z. Zhu, G. Lao, C. Ho, W. C. Campbell, and E. R. Hudson, High-resolution laser-induced fluorescence spectroscopy of $^{28}Si^{16}O^+$ and $^{29}Si^{16}O^+$ in a cryogenic buffer-gas cell, J. Mol. Spectrosc. **384**, 111582 (2022).
[38] Y. Hao, M. Iliaš, E. Eliav, P. Schwerdtfeger, V. V. Flambaum, and A. Borschevsky, Nuclear anapole moment interaction in BaF from relativistic coupled-cluster theory, Phys. Rev. A **98**, 032510 (2018).
[39] P. Filianin, C. Lyu, M. Door, K. Blaum, W. J. Huang, M. Haverkort, P. Indelicato, C. H. Keitel, K. Kromer, D. Lange, Y. N. Novikov, A. Rischka, R. X. Schüssler, C. Schweiger, S. Sturm, S. Ulmer, Z. Harman, and S. Eliseev, Direct q-value determination of the β^- decay of ^{187}Re, Phys. Rev. Lett. **127**, 072502 (2021).
[40] T. Sailer, V. Debierre, Z. Harman, F. Heiße, C. König, J. Morgner, B. Tu, A. V. Volotka, C. H. Keitel, K. Blaum, and S. Sturm, Measurement of the bound-electron g-factor difference in coupled ions, Nature (London) **606**, 479 (2022).
[41] M. Mougeot *et al.*, Mass measurements of $^{99-101}In$ challenge *ab initio* nuclear theory of the nuclide ^{100}Sn, Nat. Phys. **17**, 1099 (2021).
[42] M. Borchert, J. Devlin, S. Erlewein, M. Fleck, J. Harrington, T. Higuchi, B. Latacz, F. Voelksen, E. Wursten, F. Abbass *et al.*, A 16-parts-per-trillion measurement of the antiproton-to-proton charge–mass ratio, Nature (London) **601**, 53 (2022).
[43] L. S. Brown and G. Gabrielse, Geonium theory: Physics of a single electron or ion in a Penning trap, Rev. Mod. Phys. **58**, 233 (1986).
[44] D. Budker, D. F. Kimball, and D. P. DeMille, *Atomic Physics: An Exploration Through Problems and Solutions* (Oxford University Press, New York, 2004).
[45] S. Chattopadhyaya, A. Chattopadhyay, and K. K. Das, Electronic spectrum of SiO^+: A theoretical study, J. Mol. Struct. **639**, 177 (2003).
[46] G. Arfken, *Mathematical Methods for Physicists: Spherical Harmonics* (Academic Press, Orlando, 1985), Vol. 1, p. 680.
[47] See Supplemental Material at http://link.aps.org/supplemental/10.1103/PhysRevLett.133.033003 for a detailed investigation of the effects of time-varying electric fields as well as the derivation of the analytical formula in Eq. (1) for the parity violation asymmetry measured using the technique described in the Letter.
[48] S. B. Cahn, J. Ammon, E. Kirilov, Y. V. Gurevich, D. Murphree, R. Paolino, D. A. Rahmlow, M. G. Kozlov, and D. DeMille, Zeeman-tuned rotational level-crossing spectroscopy in a diatomic free radical, Phys. Rev. Lett. **112**, 163002 (2014).
[49] M. J. Jensen, T. Hasegawa, and J. J. Bollinger, Temperature and heating rate of ion crystals in Penning traps, J. Phys. Rev. A **70**, 033401 (2004).
[50] M. B. Comisarow and A. G. Marshall, Fourier transform ion cyclotron resonance spectroscopy, Chem. Phys. Lett. **25**, 282 (1974).
[51] R. X. Schüssler, H. Bekker, M. Braß, H. Cakir, J. R. Crespo L'opez-Urrutia, M. Door, P. Filianin, Z. Harman, M. W. Haverkort, W. J. Huang, P. Indelicato, C. H. Keitel, C. M. König, K. Kromer, M. Müller, Y. N. Novikov, A. Rischka, C. Schweiger, S. Sturm, S. Ulmer, S. Eliseev, and K. Blaum, Detection of metastable electronic states by Penning trap mass spectrometry, Nature (London) **581** (2020).
[52] A. J. Marr, M. Flores, and T. Steimle, The optical and optical/stark spectrum of iridium monocarbide and mononitride, J. Chem. Phys. **104**, 8183 (1996).
[53] P. R. Stollenwerk, I. O. Antonov, and B. C. Odom, IP determination and $1+1$ rempi spectrum of SiO at 210–220 nm in an ion trap: Implications for SiO^+ ion trap loading, J. Mol. Spectrosc. **355**, 40 (2019).
[54] X. Tong, A. H. Winney, and S. Willitsch, Sympathetic cooling of molecular ions in selected rotational and vibrational states produced by threshold photoionization, Phys. Rev. Lett. **105**, 143001 (2010).
[55] G. B. Andresen *et al.*, Evaporative cooling of antiprotons to cryogenic temperatures, Phys. Rev. Lett. **105**, 013003 (2010).
[56] S. Sturm, I. Arapoglou, A. Egl, M. Höcker, S. Kraemer, T. Sailer, B. Tu, A. Weigel, R. Wolf, J. C. López-Urrutia, and K. Blaum, The ALPHATRAP experiment, Eur. Phys. J. Spec. Top. **227**, 1425 (2019).
[57] E. Altuntaş, J. Ammon, S. B. Cahn, and D. DeMille, Measuring nuclear-spin-dependent parity violation with molecules: Experimental methods and analysis of systematic errors, Phys. Rev. A **97**, 042101 (2018).
[58] W. Chmaisani and S. Elmoussaoui, Theoretical study of laser cooling of the TlF^+ molecular ion, Phys. Chem. Chem. Phys. **23**, 1718 (2021).
[59] Y. Takeda, H. Maeda, K. Ohki, and Y. Yanagisawa, Review of the temporal stability of the magnetic field for ultra-high field superconducting magnets with a particular focus on superconducting joints between HTS conductors, Supercond. Sci. Technol. **35**, 043002 (2022).

[60] J. W. Britton, J. G. Bohnet, B. C. Sawyer, H. Uys, M. J. Biercuk, and J. J. Bollinger, Vibration-induced field fluctuations in a superconducting magnet, Phys. Rev. A **93**, 062511 (2016).
[61] C. Droese, M. Block, M. Dworschak, S. Eliseev, E. M. Ramirez, D. Nesterenko, and L. Schweikhard, Investigation of the magnetic field fluctuation and implementation of a temperature and pressure stabilization at SHIPTRAP, Nucl. Instrum. Methods Phys. Res., Sect. A **632**, 157 (2011).
[62] A. Borschevsky, M. Iliaš, V. A. Dzuba, K. Beloy, V. V. Flambaum, and P. Schwerdtfeger, Nuclear-spin-dependent parity violation in diatomic molecular ions, Phys. Rev. A **86**, 050501 (2012).
[63] K. G. Dyall, Relativistic quadruple-zeta and revised triple-zeta and double-zeta basis sets for the 4p, 5p, and 6p elements, Theor. Chem. Acc. **115**, 441 (2006).
[64] K. G. Dyall, Relativistic double-zeta, triple-zeta, and quadruple-zeta basis sets for the light elements H–Ar, Theor. Chem. Acc. **135**, 128 (2016).
[65] K. G. Dyall, Relativistic and nonrelativistic finite nucleus optimized triple-zeta basis sets for the 4p, 5p and 6p elements, Theor. Chem. Acc. **108**, 335 (2002).
[66] K. G. Dyall, Relativistic double-zeta, triple-zeta, and quadruple-zeta basis sets for the actinides Ac–Lr, Theor. Chem. Acc. **117**, 491 (2007).
[67] M. Iliaš and T. Saue, An infinite-order two-component relativistic Hamiltonian by a simple one-step transformation, J. Chem. Phys. **126**, 064102 (2007).
[68] T. Saue, Relativistic Hamiltonians for chemistry: A primer, ChemPhysChem **12**, 3077 (2011).
[69] J. V. Pototschnig, A. Papadopoulos, D. I. Lyakh, M. Repisky, L. Halbert, A. Severo Pereira Gomes, H. J. A. Jensen, and L. Visscher, Implementation of relativistic coupled cluster theory for massively parallel GPU-accelerated computing architectures, J. Chem. Theory Comput. **17**, 5509 (2021).
[70] A. Lagerqvist, I. Renhorn, and N. Elander, The spectrum of SiO in the vacuum ultraviolet region, J. Mol. Spectrosc. **46**, 285 (1973).
[71] T. Kurth, E. Berkowitz, E. Rinaldi, P. Vranas, A. Nicholson, M. Strother, and A. Walker-Loud, Nuclear parity violation from lattice QCD, Proc. Sci., LATTICE2015 (**2015**) 329.
[72] Z. Davoudi, W. Detmold, P. Shanahan, K. Orginos, A. Parreno, M. J. Savage, and M. L. Wagman, Nuclear matrix elements from lattice QCD for electroweak and beyond-standard-model processes, Phys. Rep. **700**, 1 (2021).
[73] Y. Hao, P. Navrátil, E. B. Norrgard, M. Iliaš, E. Eliav, R. G. E. Timmermans, V. V. Flambaum, and A. Borschevsky, Nuclear spin-dependent parity-violating effects in light polyatomic molecules, Phys. Rev. A **102**, 052828 (2020).
[74] E. B. Norrgard, D. S. Barker, S. Eckel, J. A. Fedchak, N. N. Klimov, and J. Scherschligt, Nuclear-spin dependent parity violation in optically trapped polyatomic molecules, Commun. Phys. **2**, 77 (2019).
[75] M. Bohman, V. Grunhofer, C. Smorra, M. Wiesinger, C. Will, M. Borchert, J. Devlin, S. Erlewein, M. Fleck, S. Gavranovic *et al.*, Sympathetic cooling of a trapped proton mediated by an LC circuit, Nature (London) **596**, 514 (2021).
[76] C. Will, M. Bohman, T. Driscoll, M. Wiesinger, F. Abbass, M. J. Borchert, J. A. Devlin, S. Erlewein, M. Fleck, B. Latacz, R. Moller, A. Mooser, D. Popper, E. Wursten, K. Blaum, Y. Matsuda, C. Ospelkaus, W. Quint, J. Walz, C. Smorra, and S. Ulmer, Sympathetic cooling schemes for separately trapped ions coupled via image currents, New J. Phys. **24**, 033021 (2022).
[77] C. Will, Image-current mediated sympathetic laser cooling of a single proton in a Penning trap down to 170 mK axial temperature, arXiv:2310.10208.
[78] W. M. Itano and D. J. Wineland, Laser cooling of ions stored in harmonic and Penning traps, Phys. Rev. A **25**, 35 (1982).
[79] S. B. Torrisi, J. W. Britton, J. G. Bohnet, and J. J. Bollinger, Perpendicular laser cooling with a rotating-wall potential in a Penning trap, Phys. Rev. A **93**, 043421 (2016).
[80] A. S. P. Gomes *et al.*, Dirac19, Zenodo, 10.5281/zenodo.3572669 (2019).
[81] T. Saue *et al.*, The Dirac code for relativistic molecular calculations, J. Chem. Phys. **152**, 204104 (2020).
[82] C. R. Harris, K. J. Millman, S. J. Van Der Walt, R. Gommers, P. Virtanen, D. Cournapeau, E. Wieser, J. Taylor, S. Berg, N. J. Smith *et al.*, Array programming with NUMPY, Nature (London) **585**, 357 (2020).
[83] P. Virtanen, R. Gommers, T. E. Oliphant, M. Haberland, T. Reddy, D. Cournapeau, E. Burovski, P. Peterson, W. Weckesser, J. Bright *et al.*, SCIPY1.0: Fundamental algorithms for scientific computing in Python, Nat. Methods **17**, 261 (2020).
[84] The Pandas Development Team, pandas-dev/pandas: Pandas, 10.5281/zenodo.10107975 (2023).
[85] Wes McKinney, Data structures for statistical computing in Python, in *Proceedings of the 9th Python in Science Conference*, edited by Stéfan van der Walt and Jarrod Millman (2010), pp. 56–61, 10.25080/Majora-92bf1922-00a.
[86] D. A. Dahl, simion for the personal computer in reflection, Int. J. Mass Spectrom. **200**, 3 (2000), volume 200: The state of the field as we move into a new millenium.
[87] J. D. Hunter, MATPLOTLIB: A 2d graphics environment, Comput. Sci. Eng. **9**, 90 (2007).